Magnetite synthesis from ferrous iron solution at pH 6.8 in a continuous stirred tank reactor

Yvonne M. Mos, Karin Bertens Zorzano, Cees J. N. Buisman and Jan Weijma

ABSTRACT

Partial oxidation of defined Fe^{2+} solutions is a well-known method for magnetite synthesis in batch systems. The partial oxidation method could serve as basis for an iron removal process in drinking water production, yielding magnetite (Fe_3O_4) as a compact and valuable product. As a first step toward such a process, a series of experiments was carried out, in which magnetite was synthesized from an Fe^{2+} solution in a 2 L continuous stirred tank reactor (CSTR) at atmospheric pressure and 32 °C. In four experiments, elevating the pH from an initial value of 5.5 or 6.0 to a final value of 6.8, 7.0 or 7.5 caused green rust to form, eventually leading to magnetite. Formation of NH_4^+ in the reactor indicated that NO_3^- and subsequently NO_2^- served as the oxidant. However, mass flow analysis revealed an influx of O_2 to the reactor. In a subsequent experiment, magnetite formation was achieved in the absence of added nitrate. In another experiment, seeding with magnetite particles led to additional magnetite precipitation without the need for a pH elevation step. Our results show, for the first time, that continuous magnetite formation from an Fe^{2+} solution is possible under mild conditions, without the need for extensive addition of chemicals.

Key words | CSTR, groundwater, iron removal, magnetite, nitrate, oxygen

Yvonne M. Mos
Karin Bertens Zorzano
Cees J. N. Buisman
Jan Weijma (corresponding author)
Sub-Department of Environmental Technology,
Wageningen University,
P.O. Box 17,
6700 AA Wageningen,
The Netherlands
E-mail: jan.weijma@wur.nl

INTRODUCTION

Groundwater is often used as a source for drinking water and can contain up to $50\ mg\ L^{-1}$ of ferrous iron. Iron removal is a necessary step in the production of drinking water, since the World Health Organization recommends an iron level of less than $0.3\ mg\ L^{-1}$ (WHO 2011). Currently, ferrous iron is usually removed by aeration, which leads to uncontrolled chemical precipitation of the resulting ferric iron, followed by sand filtration to remove the precipitates (Van Beek et al. 2016). This produces a poorly dewaterable sludge of low value (Razali et al. 2007). Alternatively, groundwater is treated by membrane filtration, resulting in a concentrate with an elevated iron concentration (Ellis et al. 2000) or by a chemical–biological process that operates at a slightly acidic pH and yields a compact iron residue (Van Beek et al. 2016).

Better controlled iron precipitation could result in more valuable and compact iron minerals like magnetite (Fe_3O_4) and reduce water losses in drinking water production. Magnetite is a black ferrous–ferric iron oxide with strong magnetic properties 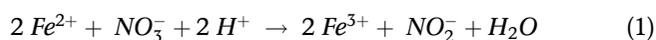at particle sizes above 20 nm (Cornell & Schwertmann 2003). These properties make magnetite particles of high purity and uniform size and shape useful in high-tech applications such as data storage, MRI techniques and site-specific chemotherapy (Laurent et al. 2008).

Conventional chemical methods to produce magnetite for such applications require high temperatures (Cornell & Schwertmann 2003; Amemiya et al. 2007; Salazar et al. 2011), high pressure and/or the addition of chemicals (e.g. for pH adjustment) (Laurent et al. 2008; Baumgartner et al. 2013a; Pereira et al. 2015; Mirabello et al. 2016), rendering these methods environmentally unfriendly, expensive and incompatible with drinking water production.
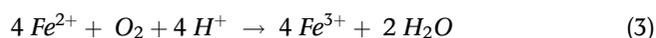
Several chemical methods for the synthesis of magnetite in water under mild conditions are known, but do not start from ferrous iron. For example, Tamaura et al. (1983) reported magnetite formation from γ-FeOOH at a minimum pH of 7.3 and 25 °C and Hansel et al. (2005) produced magnetite from ferrihydrite at pH 7 in ultra-pure water.

Here we study the partial oxidation method, originally developed by Sugimoto & Matijević (1980), for synthesis of

magnetite under groundwater-like conditions in a continuous reactor. Our ultimate aim is to develop a continuous iron removal process for ferruginous groundwater treatment, yielding magnetite as a more compact and valuable iron product. Although the partial oxidation method has been studied by several research groups to elucidate the magnetite formation mechanism, these studies were not directed at using the method as the basis for a groundwater treatment process. In the partial oxidation method, Fe^{2+} is partially oxidized to form green rust (GR) and subsequently, magnetite. NO_3^- is commonly used as the oxidant, leading to NO_2^- and eventually NH_4^+ (Chaves 2005; Matocha *et al.* 2012; Etique *et al.* 2014). Alternatively, Fe^{2+} can be oxidized by O_2, resulting in the same iron precipitation pathway (Mirabello *et al.* 2016). The (simplified) reactions involved are:

$$2\,Fe^{2+} + NO_3^- + 2\,H^+ \rightarrow 2\,Fe^{3+} + NO_2^- + H_2O \qquad (1)$$

$$8\,Fe^{2+} + NO_3^- + 10\,H^+ \rightarrow 8\,Fe^{3+} + NH_4^+ + 3\,H_2O \qquad (2)$$

Or:

$$4\,Fe^{2+} + O_2 + 4\,H^+ \rightarrow 4\,Fe^{3+} + 2\,H_2O \qquad (3)$$

Followed by:

$$Fe^{2+},\ Fe^{3+},\ H_2O \rightarrow GR \qquad (4)$$

$$Fe^{2+},\ GR \rightarrow Fe_3O_4,\ H_2O \qquad (5)$$

The formation of magnetite by this method occurs within 50 minutes to 9 hours, depending on the initial pH and Fe^{2+} concentration (1.1–28 g/L) (Sugimoto & Matijević 1980; Couling & Mann 1985; Vereda *et al.* 2013; Lenders 2015). Initial pH values range from 6 at 100 °C to 8 or 9 at room temperature (Couling & Mann 1985; Lenders 2015). Since drinking water production involves large and continuous volumes of water, any treatment process should operate continuously, under mild conditions and with little use of chemicals.

In this paper we report continuous magnetite synthesis from dissolved $FeCl_2$ at pH 6.8 in a laboratory-scale 2 L continuous stirred tank reactor (CSTR). Initially, the CSTR was fed with 50% tap water with added nitrate as the intended oxidant and 50% Milli-Q water containing 570 mg/L $FeCl_2$, as the intermediate step towards levels more typical for groundwater. In later experiments, nitrate was omitted from the tap water.

MATERIALS AND METHODS

Chemicals and analysis

All chemicals used were analytical grade. $FeCl_2$ (Alfa Aesar) was 99.5% pure, anhydrous and the container was only opened in an anaerobic hood to prevent exposure to O_2, and the $FeCl_2$ solutions were also prepared in an anaerobic hood. Nitrate was used in the form of KNO_3. All solutions were prepared using water that was purged with 99.999% pure N_2 gas (5.0 N_2, $O_2 < 5$ ppmv, Linde Gas Benelux B.V., The Netherlands) for at least 40 minutes per liter prior to use.

Soluble iron and dissolved nitrite, nitrate, and ammonium concentrations in the reactor and reactor effluent were determined with Hach Lange kits (LCK 320, LCK 339, LCK 341, LCK 305) and a DR3900 spectrophotometer (Hach Lange). The nitrate concentration in tap water was analyzed by ion chromatography (Dionex ICS 2100, Dionex IonPac AS17, $4 \times 2{,}505$ mm).

The precipitates were separated by settling and then air-dried at room temperature. This method will lead to the oxidation of any unstable Fe^{2+} present in the sample. However, magnetite is stable over a period of years and no additional magnetite can be formed in this way (Cornell & Schwertmann 2003). The precipitate samples were analyzed by X-ray diffraction (XRD) with a Bruker D2 Phaser equipped with Co radiation (300 W). A Lynxeye 1D detector was used with an incident beam slit of 1.0 mm, a diffracted beam slit of 3.0 mm and a knife at 2.0 mm above the sample holder. The sample was spun at a speed of 5.0 rpm to ensure statistically optimal results. The scanning range was 10–90° 2θ, the step size was 0.04° and the counting time per step was 2 seconds.

CSTR experiments

Table 1 lists the experiments conducted. The CSTR had a working volume of 2 L. Before the start of each experiment, the reactor was filled with 1 L Milli-Q water and 1 L local tap water from Wageningen, The Netherlands (see Table 2 for composition). A 570 mg/L $FeCl_2$ (251 mg/L Fe^{2+}) solution was prepared in Milli-Q water and a 81 mg/L KNO_3 solution was prepared in tap water.

Initially, the CSTR was fed with tap water with added KNO_3 as the intended oxidant and Milli-Q water containing 570 mg/L $FeCl_2$ at 0.028 L h^{-1} (0.67 L per day) for both, giving a hydraulic retention time of 36 hours. In later experiments, no nitrate was added to the tap water. Mixing was

Table 1 | Overview of experiments

Experiment	Inflow 1 (in Milli-Q)	Inflow 2	Initial pH	Final pH	Comment
a	570 mg/L FeCl$_2$	81 mg/L KNO$_3$ in tap water	5.5	7.5	
b	570 mg/L FeCl$_2$	81 mg/L KNO$_3$ in tap water	5.5	7.0	
c	570 mg/L FeCl$_2$	81 mg/L KNO$_3$ in tap water	5.5	6.8	initial pH elevation to 6.5
d	570 mg/L FeCl$_2$	81 mg/L KNO$_3$ in tap water	6.0	7.5	
e	570 mg/L FeCl$_2$	tap water	5.5	7.5	
f	127 mg/L FeCl$_2$	Milli-Q water	6.0	6.0	quantification O$_2$ influx
g	570 mg/L FeCl$_2$	tap water	7.0	7.0	seed crystals added at t$_0$
h	570 mg/L FeCl$_2$	tap water	5.5	7.0	step-wise procedure

Table 2 | Concentrations of ions of interest in the tap water; most concentrations were below the detection limit

Ion	Unit	Concentration
ammonium	mg NH$_4^+$ L^{-1}	<0.005
nitrite	mg NO$_2^-$ L^{-1}	<0.012
nitrate	mg NO$_3^-$ L^{-1}	0.17
ferrous iron	mg Fe^{2+} L^{-1}	<0.2
ferric iron	mg Fe^{3+} L^{-1}	<0

accomplished with a stainless steel rotor with a diameter of 4 cm and at 60 rpm in the center of the water column and magnetic stirring at approximately the same speed with a 4 cm magnetic bead placed centrally on the reactor bottom. Each experiment was conducted in a cabinet that was kept at 32 °C. The reactor was connected to a pH sensor (QP156X, QIS) and controller, which dispensed HCl (0.25 M) or NaOH (0.25 M) when the deviation from the pH set point value became greater than 0.1. Reactor, feed solutions, effluent, acid and base stocks were constantly flushed with N$_2$ gas.

We assessed the possibility of O$_2$ entering the system through the N$_2$ sparging gas (3.6 L h^{-1} in reactor and 7.2 L h^{-1} in FeCl$_2$ feed solution). The O$_2$ concentration in the sparging gas was less than 5 ppmv, so the molar mass flow into the reactor equaled no more than 3.14^*10^{-8} mol O$_2$ h^{-1}. This would account for a maximum oxidation of 7.85^*10^{-9} mol Fe^{2+} h^{-1} or 8.09^*10^{-7} mol (0.01% of total Fe^{2+} load) during a complete experiment.

Calculations and modeling

The oxidation/reduction potential (ORP) of the reactor can be calculated based on the concentrations of Fe^{2+} and Fe^{3+}, using a standard potential of 0.771 V and the Nernst

equation, as follows:

$$E = E^0 + \frac{RT}{nF}\ln\left(\frac{[ox]^i}{[red]^i}\right) \qquad (6)$$

Modeling was done with OLI Studio 9.2 (OLI Systems, Inc.).

RESULTS AND DISCUSSION

Initial tests

The reported procedure for magnetite formation with the partial oxidation method involves a pH increase (see e.g. Vereda *et al.* 2013; Altan *et al.* 2015). In trial tests (data not shown), a starting pH of around 5.5 followed by a pH elevation to 11 induced the formation of a black precipitate, which contained magnetite and no substantial amount of other mineral phases, as determined with XRD. Operating the reactor at a constant pH of either 5.5 or 7.5 did not yield magnetite precipitation.

pH limits of magnetite formation by partial oxidation in CSTR

Since our aim is to develop a process for drinking water production, the addition of pH-correcting chemicals should be kept to a minimum. We therefore conducted four CSTR experiments (see Table 1) for the following selections of initial pH and final pH: (a) pH 5.5 to 7.5, (b) pH 5.5 to 7.0, (c) pH 5.5 to 6.8, and (d) pH 6.0 to 7.5. Each experiment lasted approximately four days (103 hours). KNO$_3$ was supplied as the oxidizing agent. We increased the pH after approximately 24 hours. The color changes in the reactor content followed the same trend in experiments (a), (b) and (d). The color of the suspension in the reactor was

slightly orange at the initial pH. Following the pH increase on day 1, the suspension became dark green/brown and increasingly turbid and black during days 2 and 3. In experiment (c), however, the solution became more turbid after we increased the pH to 6.5, but the suspension remained orange. We increased the pH further to 6.8 on day 3, after which the color changed to black. We conclude that the minimum pH for magnetite formation under the applied conditions lies between pH 6.5 and 6.8. Experiment (d) had an initial pH of 6.0 and a final pH of 7.5. This procedure resulted in magnetite formation following the same trend as experiments (a) and (b), which had an initial pH of 5.5. These results demonstrate that the pH only needs a slight adjustment around circumneutral values to induce magnetite formation. The formation of magnetite was confirmed by XRD analysis for all four experiments.

Pourbaix diagram

Figure 1 shows a Pourbaix diagram for the iron phases in the CSTR.

We calculated the ORP in the reactor based on the measured concentrations of dissolved Fe^{2+}, Fe^{3+} and NO_3^- (experiment (b)) and the calculated O_2 concentration (experiment (f)) in the reactor. Based on nitrate reduction, the ORP was 0.677 V (against standard hydrogen electrode (SHE)), which is far outside the magnetite range (indicated with an asterisk in the Pourbaix diagram). However, based on O_2 reduction, the ORP was -0.496 V (vs. SHE). At pH 6.8, this is just outside of the narrow range in which magnetite is the dominant form of iron (indicated with a plus sign).

Since iron conversions other than the oxidation of Fe^{2+} also took place and the concentrations in the reactor increased over time, the actual ORP in the reactor would deviate slightly from the calculated value, allowing magnetite formation under the reactor conditions. The observed pH limit for magnetite formation in the CSTR experiments therefore correspond well with thermodynamic calculations. Although we cannot exclude the possibility that part of the ferrous iron was biologically oxidized, we consider it unlikely that this was substantial due to the low numbers of bacteria in tap water, the lack of carbon source due to CO_2 stripping, and the relatively short run time of the experiment.

Mass flow analysis of iron

We carried out a mass flow analysis for iron, for the end state of the experiments. It was based on the Fe^{2+} load, iron concentrations in the solution and precipitate concentration in both the reactor and the effluent collection vessel at the end of the experiments, assuming the precipitates to be 100% magnetite (Supporting Information Equations (1) and (2)). These calculations reveal a deviation of 2–8% in the iron balance, which we consider acceptable for a continuous process (data in Supporting Information). (The Supporting Information is available with the online version of this paper.)

Efficiency and rate of Fe^{2+} precipitation

The decrease in aqueous Fe^{2+} concentrations in the CSTR at the end of the experiments (day 4) was (a) 49%, (b) 42%, and (c) 29%, relative to the influent. Although the final pH of 7.5
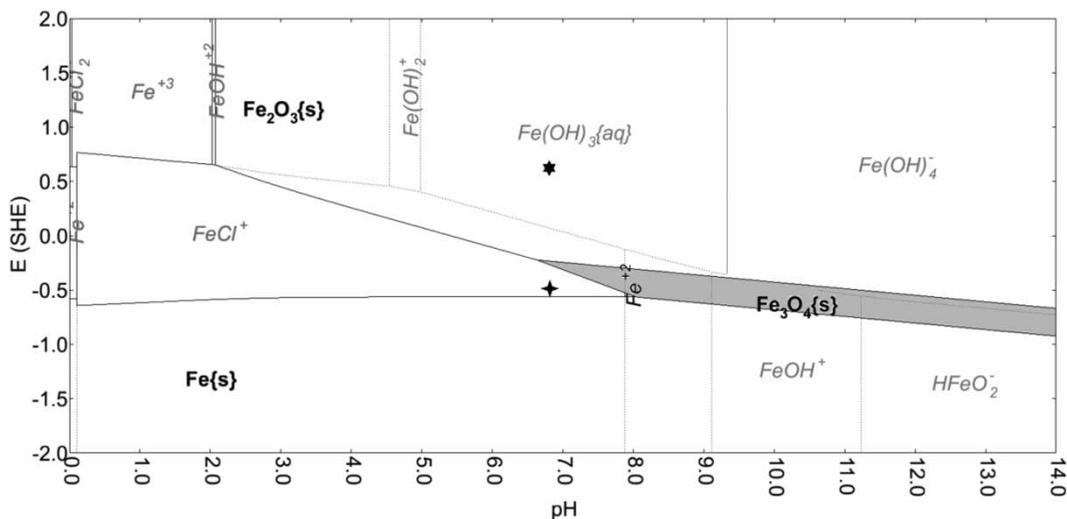

Figure 1 │ Pourbaix diagram created with OLI Studio 9.2 for the iron system; 1 mM Fe^{2+} (i.e. 55.85 mg/L, based on measurements in the reactor) and 32° C. The magnetite range is the highlighted area, * represents the reaction with NO_3^- and + represents the reaction with O_2.
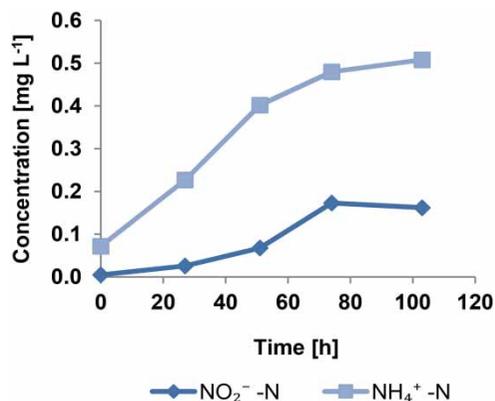
Figure 2 | Formation of nitrite and ammonium (mg L^{-1}) over time in the reactor in experiment (b).

in experiment (d) was the same as that of experiment (a), a higher fraction of iron precipitated (81%), corresponding to a rate of Fe^{2+} removal of 5.7 mg h^{-1}. The higher initial pH of 6.0 in experiment (d), compared with a pH of 5.5 for the other three experiments, apparently strongly affected the precipitation. Both the initial and the final pH therefore appear relevant for the efficiency of precipitation.

Fe^{2+}-oxidizing agents

The occurrence of reactions 1 and 2 was confirmed by the presence of nitrite and ammonium (Figure 2, showing experiment (b)). Since NH$_4^+$ is the end product of nitrate

reduction with ferrous iron (Chaves 2005; Yang & Lee 2005; Matocha *et al.* 2012) and GR (Etique *et al.* 2014), nitrite represents a mere intermediate. The standard deviation of the analytical methods was 1.5*10^{-3} mg O$_2^-$-N L^{-1} and 11.6*10^{-3} mg NH$_4^+$-N L^{-1}. Because of the higher standard deviation of the analytical method (42.9*10^{-3} mg L^{-1} for NO$_3^-$-N) and small fluctuations over time, we were unable to quantify nitrate depletion (Supporting Information, Table S6). Moreover, formation of other intermediate nitrogen compounds such as N$_2$O, as suggested by Etique *et al.* (2014), or the formation of N$_2$ cannot be excluded.

To determine to what extent nitrate reduction to nitrite and ammonium accounted for all Fe^{2+} oxidized, an electron balance was calculated for experiment (b) at day 4 (Supporting Information Equations (S3) and (S4)). The amount of iron that was oxidized was calculated based on the Fe^{2+} load, the weight of precipitates in both the reactor and the effluent per liter of total inflow and the measured Fe^{2+} in the reactor. Next to this, the amount of iron oxidation by NO$_3^-$ reduction was calculated based on the measured concentrations of NO$_2^-$ and NH$_4^+$ in the reactor according to Equations (1) and (2).

As Figure 3 shows, reduction of nitrate to nitrite and ammonium cannot account for all Fe^{2+} oxidization, indicating the presence of another oxidant in the reactor system, which can only have been O$_2$. The N$_2$ sparging gas was a source of O$_2$ (see the 'CSTR experiments' section), but this could only account for the oxidation of up to 2.32*10^{-10}

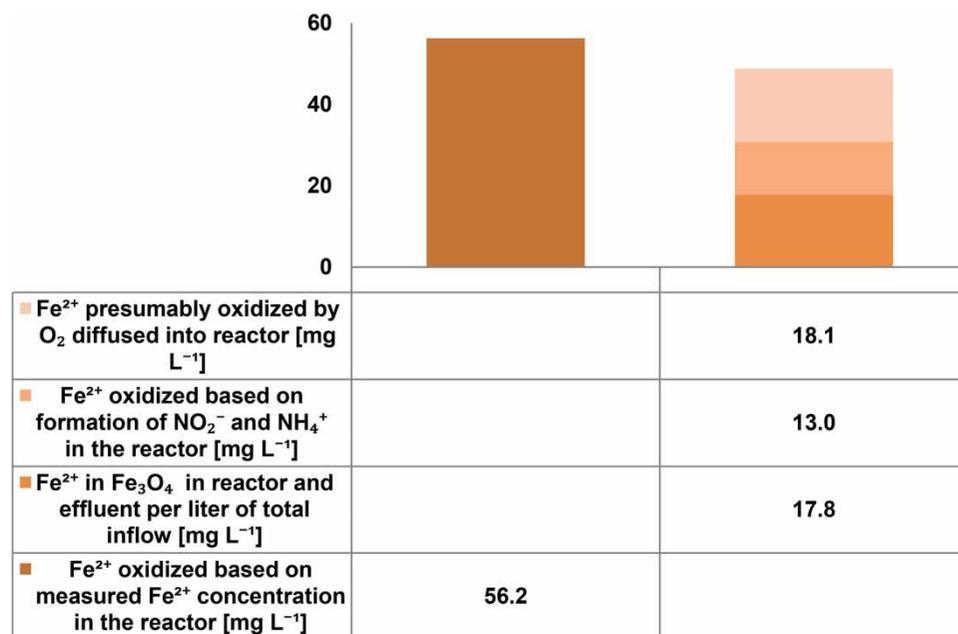|	
■ Fe^{2+} presumably oxidized by O$_2$ diffused into reactor [mg L^{-1}]	18.1
■ Fe^{2+} oxidized based on formation of NO$_2^-$ and NH$_4^+$ in the reactor [mg L^{-1}]	13.0
■ Fe^{2+} in Fe$_3$O$_4$ in reactor and effluent per liter of total inflow [mg L^{-1}]	17.8
■ Fe^{2+} oxidized based on measured Fe^{2+} concentration in the reactor [mg L^{-1}]	56.2

Figure 3 | Calculated contributions of different processes to the decrease in Fe^{2+} concentration relative to the decrease as measured directly in the reactor at the end of experiment (b). Values were calculated based on the weight of the formed precipitates per liter of total inflow and the measurements of nitrite and ammonium at the end of experiment (b) (reactions 1 and 2) and by O$_2$ diffusion as measured in experiment (f).

mg Fe^{2+}, which is only 0.1% of the total of 3.32^*10^{-7} mg Fe^{2+} (experiment (b)). Hence, we suspected diffusion of O_2 into the reactor setup, e.g. through the Teflon tubing. To confirm this, we carried out experiment (e), in which the NO_3^- feed solution was replaced with tap water without added nitrate (see Table 1 for composition). Initial (5.5) and final pH (7.5) were the same as in experiment (a). Experiment (e) yielded magnetite in a similar manner as the experiments with NO_3^-. So, although a fraction of the added nitrate is reduced, the addition of nitrate is not essential for magnetite formation. Since O_2 is more reactive with Fe^{2+}, some accumulation of nitrite is visible in the reactor. The iron precipitation was 59%, which is fairly similar to that of experiment (a) (49%) (Supporting Information).

We quantified the O_2 influx into the system in experiment (f), in which the reactor was run at a constant pH of 6 with inflow solutions of 56 mg/L Fe^{2+} in Milli-Q water and Milli-Q water without additions. No magnetite or other precipitate formed. We measured the Fe^{2+} concentration in the reactor over the course of six days. By acidifying the reactor samples to pH 3.3 ± 0.2, we ensured that all GR Fe^{2+} present was in solution before analysis. In steady state, the rate of iron oxidation was 4.88^*10^{-11} mg Fe^{2+} h^{-1} (standard deviation 2.29^*10^{-12}). This is a significant contribution (32% Fe^{2+} removal), as is clearly visible in Figure 4. The sum of the percentages of the different Fe^{2+}-removing processes adds up to an acceptable 87%.

Precipitate analysis

As stated before, magnetite formed in all experiments, except in experiment (f). However, in experiments (a)
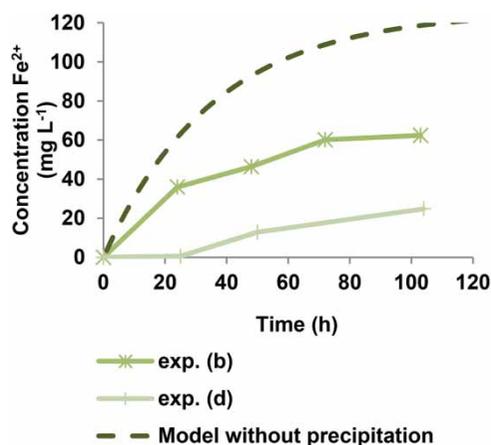

Figure 4 | Concentration of Fe^{2+} over time as calculated based on the feed and measured in experiments (b) and (d).

Table 3 | Overview of precipitates formed in experiments a, b, c and d

Experiment	pH range	Precipitates found in reactor (XRD)	Precipitates found in effluent (XRD)
a	5.5–7.5	magnetite + lepidocrocite	magnetite + lepidocrocite
b	5.5–7.0	magnetite	magnetite
c	5.5–6.8	magnetite	magnetite
d	6.0–7.5	magnetite + lepidocrocite	magnetite + lepidocrocite

and (d), lepidocrocite (γ-FeOOH) was also present in the precipitate samples from both the reactor and the effluent (see Table 3). According to Cornell & Schwertmann (2003), lepidocrocite formation is favored at a higher oxidation rate and lower Fe^{2+} concentration compared to magnetite formation. The higher final pH and lower Fe^{2+} concentrations of experiments (a) and (d) (44.4 mg L^{-1} and 24.8 mg L^{-1} respectively) therefore led to lepidocrocite formation.

Precipitation pathway

Although the experiments were not directly aimed at researching the pathway of magnetite precipitation under the applied conditions, several observations and comparisons with other studies allow some insight. The color and turbidity changes of the reactor content after increasing the pH indicate that magnetite formed from a solid phase precursor that visually resembles GR which is in agreement with what is described in the literature (Kiyama 1974; Blesa & Matijevic 1989; Cornell & Schwertmann 2003; Baumgartner *et al.* 2013b). The Fe^{2+} concentration increased over time due to the constant supply of 570 mg/L $FeCl_2$. However, the constant influx of NO_3^- and/or O_2 caused a fraction of the Fe^{2+} to precipitate immediately as is evident from the development of the concentration of dissolved Fe^{2+} (Figure 4). When we elevated the pH, the rate of increase in Fe^{2+} concentration became lower, indicating faster precipitation, which stems directly from the iron solubility at the different pH values.

To explore the mechanism of magnetite formation further, we carried out a follow-up experiment (h) with a slightly modified procedure. After a day of inflow of $FeCl_2$ and tap water at pH 5.5 in the reactor, we raised the pH to 7.0 and simultaneously stopped the inflows. The reactor content remained translucent green

throughout this phase. On day 2, we switched the inflow pumps back on. Within an hour, dark green precipitates were visible. Less than 21 hours later, the reactor had a turbid dark green to black color, becoming entirely black over time. XRD analysis confirmed magnetite formation. The green color of the reactor content points to GR having formed as the precursor for magnetite. From the well-supported dissolution–precipitation theory, it is known that Fe^{2+} in solution reacts with NO_3^- or O_2 on the surface of GR to form magnetite (Mirabello *et al.* 2016). In experiment (h), Fe^{2+} was available in the reactor, even without inflow. However, the simultaneous presence of both an unstable green precursor as well as an inflow of Fe^{2+} ions are necessary to initiate formation of magnetite.

Magnetite synthesis from seed crystals without pH elevation

As we found during our initial tests, a lower initial pH was necessary to initiate magnetite precipitation. During this phase, precipitates formed that were unstable once exposed to air, as was evident from the change in color from dark green to orange. This GR precursor appears to be essential, since no magnetite precipitated in its absence, i.e. when the reactor was run at a constant pH of 7.5. However, once the pH was raised from a lower initial value and magnetite had formed, the crystallization of magnetite continued for the three remaining days of the experiment at a constant pH of 6.8, 7.0 or 7.5.

One can hypothesize that the GR precursor that forms at the lower pH has been consumed and that the presence of already crystallized magnetite instigates further formation through the availability of surface sites (Cornell & Schwertmann 2003). To test this hypothesis, a reactor experiment (g) was conducted at a constant pH of 7; 27.7 mg L^{-1} magnetite from a previous experiment was added at the start of the experiment. No KNO_3 was supplied. Further procedures were the same as in experiments (a) to (d). This led to additional black particle formation within 24 hours. Weighing the precipitates and XRD analysis at the end of the four-day experiment showed that additional magnetite had formed. Thus, the process can be started up without pH elevation. We cannot exclude that in this experiment (g), GR also acted as the precursor for magnetite formation, although the presence of this intermediate could not be observed due to the presence of the seeding crystals. The mechanism of magnetite formation in the presence of magnetite

seeds without elevating the pH requires further attention in future work.

Implications for application

Results presented in this paper show that magnetite formation from an aqueous Fe^{2+} solution is possible in a continuous process operated at circumneutral pH and without addition of chemicals. Both aspects are important for any process intended for drinking water production. We regard this result as a first step toward application of this partial oxidation method for iron removal in drinking water production. In order to assess its application potential, numerous aspects require further research. For example, our experiments were conducted at 32 °C, whereas groundwater temperature in most areas is lower and heating is not economically feasible. Further research will have to show the possible influence of temperature on the process. We conducted our experiments in 50% diluted tap water, showing that small concentrations of other ions did not inhibit the formation of magnetite in the process. However, groundwater is a more complex medium than tap water, containing different ions often at higher concentrations. Based on our research, the presence of nitrate at concentrations typical for groundwater will not disturb the process. However, phosphate and carbonate, for example, are known to cause precipitation of vivianite and siderite respectively, rather than magnetite (Cornell & Schwertmann 2003). Further research into the effects of ions typically present in groundwater and corresponding concentrations is therefore necessary to evaluate the suitability of this process for application in drinking water production. Moreover, the process will have to be tested with the lower iron concentrations typical for groundwater. Alternatively, this process could be applied in a concentrated stream, e.g. after membrane filtration. In addition, the effect of the presence of microorganisms in a reactor will have to be evaluated. We did not consider the presence of microorganisms in our short-term experiments, but growth of microorganisms in a full-scale reactor cannot be avoided in an environmentally friendly and cost-effective manner and may be either beneficial to the process or inhibit it. Furthermore, increasing the rate and efficiency of the process is necessary to make this a viable iron removal process.

The possibilities for the application of this process are not limited to the treatment of groundwater. In the metallurgical industry, iron-rich streams are produced that result in large volumes of solid waste. Treatment of these streams

with the magnetite process might result in an additional valuable product for this industry.

CONCLUSIONS

In this paper, we have reported on the formation of magnetite in a continuous reactor from a medium based on 50% tap water and 50% Milli-Q water, at a slightly elevated temperature (32 °C), atmospheric pressure and circumneutral pH.

A series of short experiments was conducted, from which it can be concluded that O_2 caused the partial Fe^{2+} oxidation that led to the formation of magnetite. The formation of magnetite was instigated by a pH elevation from between 5.5 and 6.0 to between 6.8 and 7.5. Using a starting pH of 5.5 or slightly higher and a final pH of 7.0 (or slightly higher) suffices and may also prevent the simultaneous formation of lepidocrocite. Also, an experiment was conducted with seed crystals, revealing that seeding with magnetite particles allowed magnetite to form at a constant pH of 7, i.e. without requiring a pH change.

Since this method requires very limited addition of chemicals, it could yield a promising process for environmentally friendly iron removal in drinking water production. Further work is ongoing to explore its potential.

ACKNOWLEDGEMENTS

REFERENCES

Altan, C. L., Lenders, J. J. M., Bomans, P. H. H., De With, G., Friedrich, H., Bucak, S. & Sommerdijk, N. A. J. M. 2015 Partial oxidation as a rational approach to kinetic control in bioinspired magnetite synthesis. *Chemistry – A European Journal* **21** (16), 6150–6156. doi:10.1002/chem.201405973.

Amemiya, Y., Arakaki, A., Staniland, S. S., Tanaka, T. & Matsunaga, T. 2007 Controlled formation of magnetite crystal by partial oxidation of ferrous hydroxide in the presence of recombinant magnetotactic bacterial protein mms6. *Biomaterials* **28** (35), 5381–5389. doi:10.1016/j.biomaterials. 2007.07.051.

Baumgartner, J., Bertinetti, L., Widdrat, M., Hirt, A. M. & Faivre, D. 2013a Formation of magnetite nanoparticles at low temperature: from superparamagnetic to stable single domain particles. *PLOS ONE* **8** (3). doi:10.1371/journal. pone.0057070.

Baumgartner, J., Dey, A., Bomans, P. H. H., Le Coadou, C., Fratzl, P., Sommerdijk, N. A. J. M. & Faivre, D. 2013b Nucleation and growth of magnetite from solution. *Nature Materials* **12** (4), 310–314. doi:10.1038/nmat3558.

Blesa, M. A. & Matijevic, E. 1989 Phase transformations of iron oxides, oxohydroxides, and hydrous oxides in aqueous media. *Advances in Colloid and Interface Science* **29** (3–4), 173–221. doi:10.1016/0001-8686(89)80009-0.

Chaves, L. H. G. 2005 The role of green rust in the environment: a review. *Revista Brasileira de Engenharia Agrícola E Ambiental* **9** (2), 284–288. doi:10.1590/S1415-43662005000200021.

Cornell, R. M. & Schwertmann, U. 2003 *The Iron Oxides – Structure, Properties, Reactions, Occurrences and Uses,* 2nd edn. WILEY-VCH, Weinheim, Germany.

Couling, S. B. & Mann, S. 1985 The influence of inorganic phosphate on the crystallization of magnetite (Fe3O4) from aqueous solution. *J. Chem. Soc., Chem. Commun.* **1**, 1713–1715.

Ellis, D., Bouchard, C. & Lantagne, G. 2000 Removal of iron and manganese from groundwater by oxidation and microfiltration. *Desalination* **130**, 255–264. doi:10.1016/ S0011-9164(00)00090-4.

Etique, M., Zegeye, A., Grégoire, B., Carteret, C. & Ruby, C. 2014 Nitrate reduction by mixed iron(II-III) hydroxycarbonate green rust in the presence of phosphate anions: the key parameters influencing the ammonium selectivity. *Water Research* **62**, 29–39. doi:10.1016/j.watres.2014.05.028.

Hansel, C. M., Benner, S. G. & Fendorf, S. 2005 Competing Fe(II)-Induced mineralization pathways of ferrihydrite. *Environmental Science & Technology* **39** (18), 7147–7153. doi:10.1021/es050666z.

Kiyama, M. 1974 Conditions for the formation of Fe3O4 by the Air oxidation of Fe(OH)$_2$ suspensions. *Bulletin of the Chemical Society of Japan* **47** (7), 1646–1650. http://pdf. lookchem.com/pdf/22/198f5b73-e9c1-4007-bc23-bdbd315282a4.pdf.

Laurent, S., Forge, D., Port, M., Roch, A., Robic, C., Vander Elst, L. & Muller, R. N. 2008 Magnetic iron oxide nanoparticles: synthesis, stabilization, vectorization, physicochemical characterizations, and biological applications. *Chem. Rev.* **108** (June), 2064–2110. doi:10.1021/cr068445e.

Lenders, J. J. M. 2015 *Biomimetic Macromolecule-Mediated Magnetite Mineralization.* Technische Universiteit Eindhoven, Eindhoven, The Netherlands.

Matocha, C. J., Dhakal, P. & Pyzola, S. M. 2012 The role of abiotic and coupled biotic/abiotic mineral controlled redox processes in nitrate reduction. In: *Advances in Agronomy*, D. Sparks (ed.), Vol. 115, 1st edn. Elsevier Inc., San Diego, USA, pp. 181–214. doi:10.1016/B978-0-12-394276-0.00004-4.

Mirabello, G., Lenders, J. J. M. & Sommerdijk, N. A. J. M. 2016 Bioinspired synthesis of magnetite nanoparticles. *Chem. Soc. Rev.* **45**, 5085–5106. doi:10.1039/C6CS00432F.

Pereira, C., Pereira, A. M., Rocha, M., Freire, C. & Geraldes, C. F. G. C. 2015 Architectured design of superparamagnetic Fe_3O_4 nanoparticles for application as MRI contrast agents: mastering size and magnetism for enhanced relaxivity. *Journal of Material Chemistry B* **3**, 6261–6273. doi:10.1039/C5TB00789E.

Razali, M., Zhao, Y. Q. & Bruen, M. 2007 Effectiveness of a drinking-water treatment sludge in removing different phosphorus species from aqueous solution. *Separation and Purification Technology* **55**, 300–306. doi:10.1016/j.seppur.2006.12.004.

Salazar, J. S., Perez, L., De Abril, O., Truong Phuoc, L., Ihiawakrim, D., Vazquez, M., Greneche, J.-M., Begin-Colin, S. & Pourroy, G. 2011 Magnetic iron oxide nanoparticles in 10 - 40 Nm range: composition in terms of magnetite/maghemite ratio and effect on the magnetic properties. *Chemistry of Materials* **23**, 1379–1386.

Sugimoto, T. & Matijević, E. 1980 Formation of uniform spherical magnetite particles by crystallization from ferrous hydroxide gels. *Journal of Colloid And Interface Science* **74** (1), 227–243. doi:10.1016/0021-9797(80)90187-3.

Tamaura, Y., Ito, K. & Katsura, T. 1983 Transformation of Y-FeO(OH) to Fe_3O_4 by adsorption of iron-II ion on Y-FeO(OH). *Journal of the Chemical Society. Dalton Transactions* **2**, 189–194.

Van Beek, C. G. E. M., Dusseldorp, J., Joris, K., Huysman, K., Leijssen, H., Schoonenberg Kegel, F., De Vet, W. W. J. M., Van de Wetering, S. & Hofs, B. 2016 Contributions of homogeneous, heterogeneous and biological iron(II) oxidation in aeration and rapid sand filtration (RSF) in field sites. *Journal of Water Supply: Research and Technology – AQUA* **65** (3), 195–207. doi:10.1017/CBO9781107415324.004.

Vereda, F., de Vicente, J. & Hidalgo-Alvarez, R. 2013 Oxidation of ferrous hydroxides with nitrate: a versatile method for the preparation of magnetic colloidal particles. *Journal of Colloid and Interface Science* **392** (1), 50–56. doi:10.1016/j.jcis.2012.09.064.

WHO 2011 *Guidelines for Drinking-Water Quality*.

Yang, G. C. C. & Lee, H.-L. 2005 Chemical reduction of nitrate by nanosized iron: kinetics and pathways. *Water Research* **39**, 884–894. doi:10.1016/j.watres.2004.11.030.